

Laser-Derived, Particle Size Data from CRP-2/2A: Implications for Sequence and Seismic Stratigraphy

K.J. WOOLFE^{1†}, L.K. STEWART¹, C.R. FIELDING² & M. LAVELLE³

¹School of Earth Sciences, James Cook University, Townsville, Queensland 4811, Australia

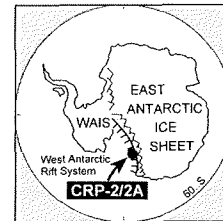
²Department of Earth Sciences, University of Queensland, Qld 4072, Australia (chrisf@earthsciences.uq.edu.au)

³British Antarctic Survey, High Cross, Madingley Road, Cambridge CB3 0ET, United Kingdom

[†]Deceased

Received 23 February 1999; accepted in revised form 6 September 2000

Abstract - Gravel-free, high-resolution (1-metre spacing, 32 channel) particle size data from the CRP-2/2A drill core indicate that many of the diamictites were likely deposited from floating ice. Textural dislocations occur at most sequence boundaries and provide independent corroboration of the sequence stratigraphic interpretation. Likewise the data largely support the correlation drawn (Fielding et al., this volume) between the sequence stratigraphic cycles and the regional seismic stratigraphy (an alternative correlation to Reflector 'f' is also suggested). The gravel-free data appear to be reflecting predominantly regional (global?) forcing with some possible local effects, and long-term trends persisting through gravelly textural dislocations.



INTRODUCTION

We report preliminary results from a study of down-hole particle size variation in the CRP-2/2A drill cores. The data are derived by the same method as those reported by Woolfe et al. (1998) from CRP-1 and by Fielding et al. (1997) from CIROS-1, and are designed to be used as part of the stratigraphic analysis of Cape Roberts Project drillholes. Trends in grain-size over vertical intervals of tens of metres are readily discernible, along with some larger-scale variations: these can be used to test hypotheses concerning stratigraphic architecture, correlation of CRP-2/2A with seismic stratigraphy and with other Cape Roberts Project drillholes.

METHODS

Samples (1 cm³) were collected at approximately one-metre intervals throughout the core from material judged visually to be representative of the local lithology, and were analysed using standard laser diffraction. Sample preparation and analysis was conducted using the methodology employed for CRP-1 (Woolfe et al., 1998). However, a hardware fault (cabling) resulted in data loss in 3 of the 32 class intervals (channels) for some samples. This caused zero values to be returned for channels 18, 19 and 20, which record particles of fine sand size (108-195 microns).

The missing channels were interpolated using a computer program written in the Visual Basic programming language. The raw particle size data are reported as relative volumes. Within the data, each class-interval is represented by a single value, that of the interval's upper boundary. The set of class-intervals is represented by a sequence of values that, due to their logarithmic distribution, are

unevenly spaced. Newton's method of divided differences allows an interpolating polynomial, $P(x)$, to be constructed from a set of n points $\{x_i, f(x_i)\}$, where the x_i are unevenly spaced (Hultquist, 1988). Consequently, this was the chosen method of interpolation.

The interpolating polynomial $P(x)$ will pass through the set of points $\{x_i, f(x_i)\}$ and when evaluated at some point, x , that does not belong to the set of points $\{x_i\}$, will provide an interpolated value of $f(x)$. The values that are produced using this method of interpolation will vary with the degree of $P(x)$. Therefore, several interpolating polynomials of degree 2, and higher, were evaluated in order to determine the one most likely to provide interpolated data that are, generally, representative of the missing information.

Approximately 60 percent of the grain size analyses were unaffected by missing data. These analyses were used to determine the degree of $P(x)$ that was likely to give the best interpolation of the missing data. A subset, $\{A\}$, of these analyses (204) was modified by removing data from the three class-intervals for which bad data were returned in some analyses. With respect to each member of $\{A\}$ the values of relative volume for each of these class intervals was then interpolated using a sequence of interpolating polynomials, of differing degrees. An interpolating polynomial of degree 2 was found to be the most effective, producing a mean (across all members of $\{A\}$) relative cumulative-error of the interpolated values, with respect to the "actual" values, of the order of -1.5% . Thus, the data missing due to the hardware fault was interpolated using an interpolating polynomial of degree 2.

We also remind readers that laser-derived particle diameters need not be directly equivalent to those derived from sieve and/or X-ray estimation of equivalent spherical settling diameters (e.g. Sedigraph data: compare the data of De Santis & Barrett, 1998 with those of Woolfe et al.,

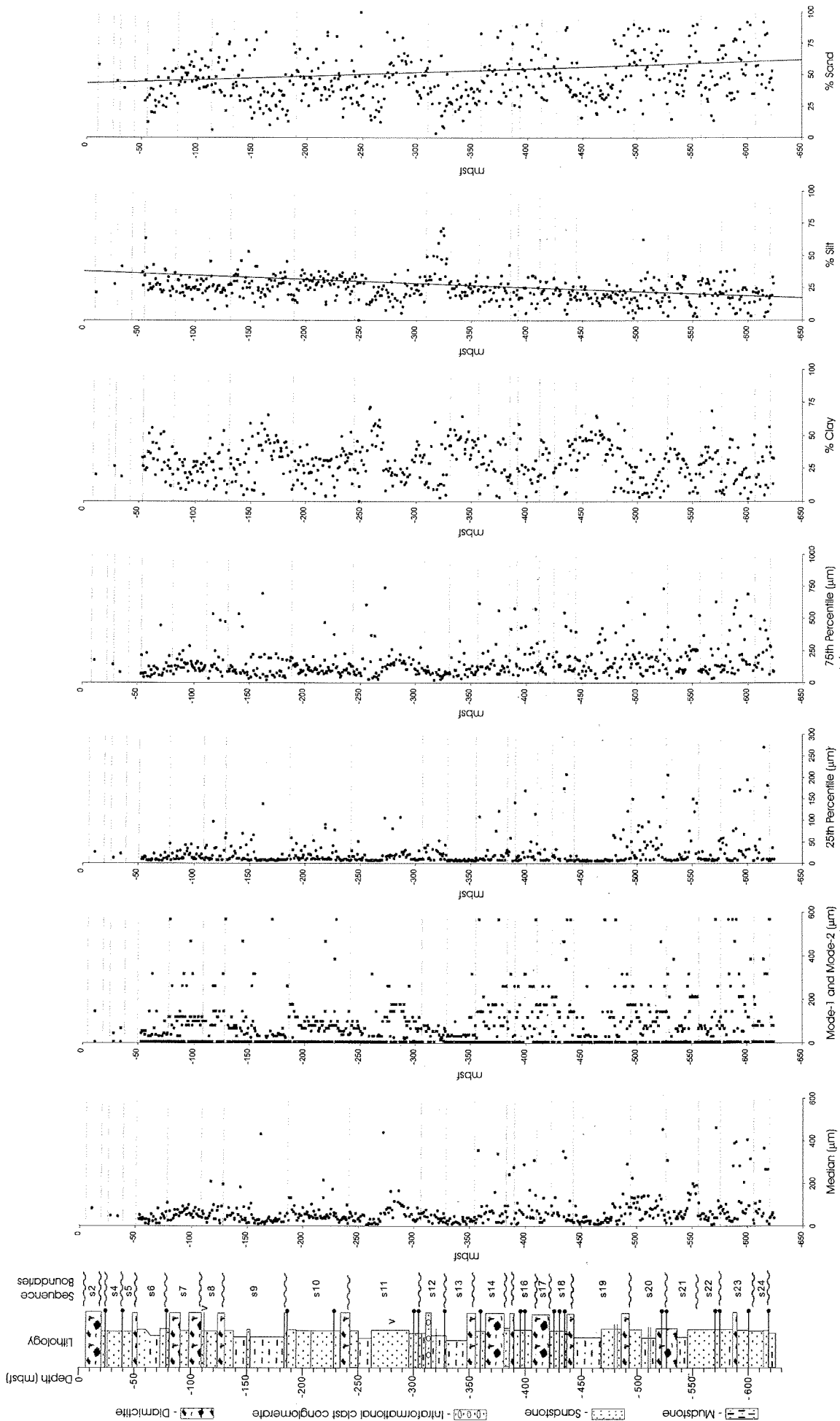


Fig. 1 - Down-hole variability in laser diffraction particle size parameters - median (d50), primary and secondary mode (M1 & M2), 25th percentile (d25), 75th percentile (d75), all percentiles and modes expressed in µm), % clay (*finer than 12 mm laser diffraction diameter), % silt (* lower boundary placed at 12 mm laser diffraction diameter) and % sand. Horizontal lines are sequence boundaries (see Fielding et al. this volume, and Table 1).

1998). Differences can be expected to result from shape functions (all methods), non-Newtonian settling at moderate concentrations (Sedigraph), and interference of diffracted rays (in laser system). A comparison between laser diffraction and sieve/Sedigraph data for CRP-2/2A is presented by Barrett et al. (this volume). The above notwithstanding, we have demonstrated (Woolfe et al., 1998) a high degree of internal consistency in our data, but may not claim that it is a better or worse representation of the true grain-sized distribution of a sample than that provided by any other method.

RESULTS

Corrected (interpolated) data together with a range of derived parameters were exported into an Excel spreadsheet and graphed in the depth (mbsf) domain (Fig. 1). Pre-Quaternary sequence boundaries (after Cape Roberts Science Team, 1999 and Fielding et al., this volume: see Tab. 1) were incorporated into the data set as an additional series and linked by trend lines.

The data show considerable scatter (Fig. 1). However, there is a progressive down-hole increase in the amount of sand and a corresponding decrease in silt content. Downward coarsening of the median (d50), primary mode (M1) and secondary mode (M2) also reflect this trend. Textural variability on a sequence scale is summarised in table 2 and figure 1.

Many of the sequences show coarsening upward trends (7, 9, 10, 12, 16, 17, 18, 22, and 23) while some display fining upward characteristics (5, 6, 8, 13, 19, and 21). Two sequences (11 and 19) show fining- and coarsening-

upward trends. The remaining sequences (14, 15, 20, and 24) show no clear trends. Textural dislocations are evident at most sequence boundaries.

DISCUSSION

Since a number of datasets have been shown to exhibit close correlation with the sequence stratigraphic subdivision of both CRP-1 and -2/2A (Cape Roberts Science Team 1998, 1999), it is tempting to interpret the textural changes described above in terms of a conventional sequence stratigraphic framework. In this framework, the finer-grained intervals might be related to highstand systems tracts (HSTs) and the coarser-grained facies to transgressive systems tracts (TST's) and regressive systems tracts (RST's). However, the data presented are gravel-free and the stratigraphic succession contains significant gravelly intervals (diamictites and conglomerates). In lower latitude, non-glaciated shelf settings, gravelly sediments are commonly sandy and consequently textural trends in gravel-free analyses may serve as a good proxy for the bulk sediment. This relationship does not appear to be reflected in the data acquired from CRP-2/2A. Gravelly diamictites at the base of sequences are commonly finer-grained (on a gravel-free basis) than the overlying sandy mudstone or sandstone (e.g. Sequences 10 and 11).

The persistence of long wavelength (gravel-free) textural trends (in the depth domain) through intervals containing diamictites suggests that the diamictite may have resulted from the addition of a coarse-fraction (gravel) to a systematically evolving (i.e. fining or coarsening)

Tab. 2 - Textural trends identified in pre-Quaternary sequences (sequences 5-24: see Fielding et al. this volume, and Tab. 1).

Sequence Number	Textural Characteristics
5	Very weak upward fining: D(75) D(50), D(25), %clay, %silt, %sand.
6	Weak upward fining: D(75), D(50), %clay, %silt, %sand.
7	Upward coarsening: D(75), D(50), D(25), %clay, %sand.
8	No clear trends, ?very weak fining: D(50).
9	Coarsening upwards: D(75), D(50), D(25), M1+2, %clay, %sand.
10	Coarsening upwards: D(75), D(50), D(25), M1+2, %clay, %silt, %sand.
11	Coarsening upward, then fining upward, then weak coarsening up. Strong coarsening event c. 280 mbsf: D(75), D(50), D(25), M1+2, %clay, %silt, %sand
12	Coarsening upwards, strong dislocation at base, with overlying silt peak: D(75), D(50), D(25), M1+2, %clay, %silt, %sand
13	Weak fining upwards: D(75), D(50), D(25), M1+2, %clay, %silt, %sand
14	No clear trends.
15	No clear trends
16	Coarsening upwards: D(75), D(50), %clay, %sand.
17	Coarsening upwards: D(75), D(50), %clay, %sand.
18	Coarsening upwards: D(75), D(50), %clay, %sand.
19	Fining then coarsening upwards: D(75), D(50), D(25), M1+2, %clay, %sand.
20	No clear trend, ?very weak coarsening: D(50).
21	Fining upwards: D(75), D(50), D(25), M1+2, %clay, %silt, %sand
22	Weak, coarsening up, scatter at base: D(50), D(25), %sand.
23	Weak, coarsening up, scatter at base: D(50), D(25), %sand.
24	No clear trend.

Tab. 1 - Depth and lithostratigraphic location of sequence boundaries in the CRP-2A drill core (from Cape Roberts Science Team, 1999).

Sequence Number	Lithostratigraphic Position of Base	Depth at Base of Sequence
4	base of Unit 4.1	52.3 m
5	within Unit 6.1	80.70 m
6	base of Unit 6.2	90.67 m
7	base of Unit 7.1	109.07 m
8	base of Unit 8.1	130.27 m
9	base of Unit 9.1	185.96 m
10	base of Unit 9.5	242.70 m
11	base of Unit 10.1	306.65 m
12	base of Unit 11.2	327.43 m
13	within Unit 12.1	362.8 m
14	base of Unit 12.1	379.0 m
15	within Unit 12.2	396.6 m
16	within Unit 12.3	408.96 m
17	base of Unit 12.3	419.88 m
18	base of Unit 12.	442.99 m
19	base of Unit 13.	493.00 m
20	within Unit 14.1	525.23 m
21	within Unit 15.2	554.64 m
22	base of Unit 15.2	574.20 m
23	base of Unit 15.4	601.53 m
24	base of Unit 15.5	614.56 m

Tab. 3 - Proposed correlation between textural parameters (Fig. 1), and trends (Tab. 2) with local and regional seismic reflectors (see also Fielding et al., this volume, Henrys et al., this volume).

Reflector	Sequence Boundary	Textural characteristics	Alternative Correlation
oc	base-6	S7 coarser than S6 and S5	base-6
D	base-8	S9 is generally finer than S8	base-8
Un-named (a)	base-9	Top of coarsening trend	base-9
F	mid-10	?	
F		Top of coarsening trend	base-10
Un-named (b)	base-10	Top of coarsening trend	
Un-named (b)		Coarse-grained event	mid-11
I	base-11	Top of coarsening trend	base-11
1 (V4/V5)	base-18	Base of coarsening trend	base-18

sedimentary environment. This may provide indirect evidence of deposition from floating rather than grounded ice. Moreover, the development of coarsening-upwards trends immediately above sequence boundaries (or glacial surfaces of erosion: GSE's – see Cape Roberts Science Team, 1998, 1999, Fielding et al., 1998, this volume) may reflect relative sea-level fall during glacial retreat. This could be the product of a local glacioisostatic response to unloading, after overdeepening of the glaciated margin during formation of the GSE. The persistence of these long wavelength trends also suggests that gravel-free textural data may prove direct evidence of global forcing, insofar as local factors (*e.g.* advance of an ice-shelf or grounded ice-sheet) appear to be partially filtered by excluding gravel from the analysis. Zones of scattered data, nonetheless, may indicate periods when more local factors were dominant.

Fielding et al. (this volume) correlate a number of their sequence boundaries with the seismic reflectors identified by Henrys et al. (this volume). These correlations together with a summary of the textural discontinuities associated with the boundaries are summarised in table 3. All of the identified sequence boundary-reflector correlations correspond to textural changes in the core. Seismic reflector 'f' which Fielding et al. (this volume) place in the middle of Sequence 10 is not picked on the basis of the textural data presented here. However, a strong mid-sequence coarsening event occurs in sequence 11 and this is not currently correlated with an identified reflector. This poses an alternative interpretation in which reflector 'f' may be correlated with the base of Sequence 10 and the underlying un-named reflector might then correspond to the coarsening event recorded near the middle of Sequence 11.

CONCLUSIONS

Gravel-free, laser-derived particle size data from the CRP-2/2A cores show good correlation with both seismic and stratigraphic sequences. Particle-size trends (on a

gravel-free basis) persist uninterrupted through many of the diamictic units, suggesting that those diamictites were probably deposited from floating ice (although other diamictites may record grounded ice over the drillsite: Cape Roberts Science Team, 1999). Moreover, the persistence of textural trends through entire sequence stratigraphic units indicates that the data might yield useful environmental forcing information (see Woolfe et al., 1998, Naish et al., this volume).

ACKNOWLEDGEMENTS

Australian participation in the Cape Roberts project was supported by Large Grants from the Australian Research Council to KJW & CRF, and by James Cook University, the University of Queensland and the Department of Industry, Science and Tourism. Constructive reviews of the submitted manuscript were provided by E.A. Cowan and S.J. Kluiving.

REFERENCES

- Cape Roberts Science Team, 1998. Miocene strata in CRP-1, Cape Roberts Project Antarctica. *Terra Antartica*, **5**(1), 63-124.
- Cape Roberts Science Team, 1999. Initial Investigations of the CRP-2 drillhole, Cape Roberts Project Antarctica. *Terra Antartica*, **6**(1/2), 1-173.
- DeSantis L. & Barrett P.J., 1998. Grain size analysis of samples from CRP-1. *Terra Antartica*, **5**, 375-382.
- Fielding C.R., Woolfe K.J., Purdon R.G., Howe J.A. & Lavelle M.A., 1997. Sedimentological and sequence stratigraphic re-evaluation of the CIROS-1 core, McMurdo Sound, Antarctica. *Terra Antartica*, **4**(2), 149-160.
- Fielding C. R., Woolfe K. J., Howe J. A & Lavelle M., 1998. Sequence stratigraphic analysis of CRP-1, Cape Roberts Project, McMurdo Sound, Antarctica. *Terra Antartica*, **5**(3), 353-362.
- Hultquist P. F., 1988. *Numerical methods for engineers and computer scientists*. Benjamin/Cummings Publishing, California, 326pp.
- Woolfe K. J., Fielding C. R., Howe J. A & Lavelle M., 1998. Laser-derived particle size characterisation of CRP-1, McMurdo Sound, Antarctica. *Terra Antartica* **5**(3), 383-392.